© 2016. Published by The Company of Biologists Ltd | Development (2016) 143, 3742-3750 doi:10.1242/dev.130427

RESEARCH ARTICLE

Adaptive protein divergence of BMP ligands takes place under developmental and evolutionary constraints

Petra M. Tauscher, Jinghua Gui and Osamu Shimmi*

ABSTRACT

The bone morphogenetic protein (BMP) signaling network, comprising evolutionary conserved BMP2/4/Decapentaplegic (Dpp) and Chordin/Short gastrulation (Sog), is widely utilized for dorsal-ventral (DV) patterning during animal development. A similar network is required for posterior crossvein (PCV) formation in the *Drosophila* pupal wing. Although both transcriptional and post-transcriptional regulation of co-factors in the network gives rise to tissue-specific and species-specific properties, their mechanisms are incompletely understood. In *Drosophila*, BMP5/6/7/8-type ligands, Screw (Scw) and Glass bottom boat (Gbb), form heterodimers with Dpp for DV patterning and PCV development, respectively. Sequence analysis indicates that the Scw ligand contains two N-glycosylation motifs: one being highly conserved between BMP2/4- and BMP5/6/7/8-type ligands, and the other being Scw ligand specific. Our data reveal that N-glycosylation of the Scw ligand boosts BMP signaling both in cell culture and in the embryo. In contrast, N-glycosylation modifications of Gbb or Scw ligands reduce the consistency of PCV development. These results suggest that tolerance for structural changes of BMP5/6/7/8-type ligands is dependent on developmental constraints. Furthermore, gain and loss of N-glycosylation motifs in conserved signaling molecules under evolutionary constraints appear to constitute flexible modules to adapt to developmental processes.

KEY WORDS: *Drosophila*, N-glycosylation, Protein evolution, Bone morphogenetic protein (BMP), Patterning, Post-transcriptional regulation

INTRODUCTION

The bilaterian body plan repeatedly utilizes highly conserved molecular mechanisms known as genetic toolkits (Carroll, 2008; De Robertis, 2008). The molecules in these toolkits include several growth factors such as bone morphogenetic protein (BMP), epidermal growth factor (EGF), fibroblast growth factor (FGF), Hedgehog, Notch and Wnt/wingless (Wg). Addressing how diversified structures are generated by conserved mechanisms is a fundamental question in biology. Changes in gene regulatory networks have been considered as major sources of novelty during development among species (Carroll, 2008; Peter and Davidson, 2011). In fact, it has been shown that changes in expression patterns of growth factors give rise to morphological novelty (Abzhanov et al., 2004; Werner et al., 2010). However, less is known about how 'conserved' growth factors bring about distinct functions through changes in the intrinsic properties of the ligand (Dickinson et al., 2011).

Institute of Biotechnology, University of Helsinki, Helsinki 00014, Finland.

*Author for correspondence (osamu.shimmi@helsinki.fi)

O.S., 0000-0001-6341-9130

Received 02 September 2015; Accepted 17 August 2016

Dorsal-ventral (DV) patterning during early embryogenesis in Bilateria and directed axis formation in Cnidaria, an outgroup of Bilateria, are regulated by a conserved BMP network comprising BMP2/4/Decapentaplegic (Dpp) and the BMP binding proteins Chordin/Short gastrulation (Sog) (De Robertis, 2008). Pioneering work in *Xenopus* and *Drosophila* indicated that BMP2/4/Dpp and Chordin/Sog are expressed at the opposite ends of the body axis to establish DV patterning (De Robertis and Sasai, 1996; De Robertis, 2008). Further studies led to a refinement of this concept. In *Xenopus* embryos, the dorsal half is self-regulated without BMP4/7 expression, as the BMP activity gradient is re-established through increased anti-dorsalizing morphogenetic protein (ADMP) activity (Reversade and De Robertis, 2005). In sea urchin, an echinoderm, Nodal signal regulates both *bmp2/4* and *chordin* expression at the ventral side of the embryo, which then induce BMP signaling at the dorsal side (Lapraz et al., 2009). In the Cnidarian *Nematostella*, *dpp* and *chordin* are co-expressed for directive axis patterning to induce BMP signaling at the opposite side of the axis (Genikhovich et al., 2015). Furthermore, BMP morphogen gradient in the mosquito *Anopheles gambiae* embryo is formed in a different manner from that in the *Drosophila* embryo, an observation attributed to changes in *sog* expression (Goltsev et al., 2007). Taken together, these facts illustrate that spatial information of *chordin/sog* expression instructs positional information of BMP signaling for DV patterning, but not BMP expression patterns per se (Bier and De Robertis, 2015).

In addition to core components of the BMP network, various co-factors have been implicated in DV patterning. These components appear to have been gained and lost throughout evolution and provide species-specific properties. In the Arthropoda lineage, it has been proposed that ADMP was lost after Hymenoptera divergence, and *tolloid* (*tld*) and *twisted gastrulation* (*tsg*) were duplicated prior to the origin of Diptera (Van der Zee et al., 2008). The BMP5/6/7/8 (BMP5-8)-type ligand Screw (Scw), an essential co-factor that forms a heterodimer with Dpp for embryonic DV patterning in *Drosophila* (Shimmi et al., 2005b; Shimmi and Newfeld, 2013), is only found in higher Diptera. A recent study suggests that the *scw* gene originated between the separation of the lineage leading to Brachycera and the origin of Cyclorrhapha through the duplication of another BMP5-8 gene, *glass bottom boat* (*gbb*), which is commonly found throughout the Arthropoda lineage (Wotton et al., 2013). Functional analysis in the scuttle fly *Megaselia abdita* suggests that both Gbb and Scw are utilized as co-factors of the BMP network for DV patterning (Rafiqi et al., 2012). In *Drosophila*, *gbb* expression is not observed in the early embryo, but Gbb plays a crucial role in posterior crossvein (PCV) formation during the pupal stage, at which an analogous mechanism utilizing a Gbb:Dpp heterodimer is needed for BMP signaling (Shimmi et al., 2005a; Matsuda and Shimmi, 2012; Shimmi and Newfeld, 2013). Intriguingly, it has been found that Scw can restore the wild-type phenotype in crossveinless

Development (2016) 143, 3742-3750 doi:10.1242/dev.130427

gbb mutant wings, whereas Gbb cannot replace Scw in the early embryo (Fritsch et al., 2010; Matsuda and Shimmi, 2012). Therefore, as co-factors of the BMP network, the paralogs Gbb and Scw provide a unique model to understand protein divergence of signaling molecules.

In this study, we show a highly conserved N-glycosylation motif in the BMP2/4 and BMP5-8 type ligands, and a motif unique to the Scw ligand. Our results in cell culture and *in vivo* suggest that both N-glycosylation motifs in the Scw ligand are needed for peak-level BMP signaling in the embryo, whilst Gbb is unable to participate in embryonic DV patterning. Although both Gbb and Scw are capable of contributing to PCV development, the presence of N-glycosylation motifs in the Gbb or Scw ligands do not confer an advantage during PCV formation, but rather decrease developmental consistency during PCV development. Therefore, our data suggest that different developmental and evolutionary constraints provide context specificity among highly conserved signaling molecules and homologous pathways.

RESULTS

N-glycosylation motifs among the BMP2/4 and BMP5-8 type ligands

Previous studies address the question of how the Scw and Gbb ligands are differentially utilized for developmental processes in different contexts (Fritsch et al., 2010; Matsuda and Shimmi, 2012). Since both proteins are categorized as BMP5-8 type ligands, we wondered whether changes in protein structure can affect the respective signaling activities of Gbb and Scw. One such change could be caused by post-transcriptional modifications such as N-glycosylation. It has been shown that N-glycosylation of BMP6 has an impact on its signaling *in vitro* (Saremba et al., 2008). However, the acquisition of N-glycosylations in TGF-β type ligands and their impact on signaling *in vivo* largely remains to be addressed. A sequence alignment and phylogenetic analysis of various ligands belonging to the TGF-β family reveal a highly conserved N-glycosylation motif (N-[X]-[S/T]), in which X represents any amino acid except proline, among the BMP2/4 and BMP5-8 type ligands (Fig. 1, Fig. S1). Interestingly, the Scw ligands reveal an additional motif in the N-terminal region of the ligand domain (Fig. 1 and Fig. S1B) (Arora et al., 1994). Among the analyzed TGF-β type ligands, human and mouse GDF3 have an N-glycosylation motif at the position homologous to BMP2/4 and BMP5-8 type ligands (Fig. 1, Fig. S1). These facts suggest that an N-glycosylation motif has been acquired prior to divergence of BMP2/4, BMP5-10, GDF1/3 and GDF5-7, then lost after GDF1, GDF5-7 and BMP9/10 divergence, and gained at the unique site after Scw divergence. Taken together, these findings suggest that N-glycosylation sites in the TGF-β type ligands might have been repeatedly gained and lost throughout evolution.

N-glycosylation in the Scw ligand impacts BMP signaling in *Drosophila* S2 cells

The sequence analysis of the Scw and Gbb ligand domains poses of the following questions: are they indeed N-glycosylated? If so, does N-glycosylation of ligands affect signaling? First, to elucidate whether the two N-glycosylation motifs in the Scw ligand domain are utilized, prospective N-glycosylation sites were mutated by site-specific mutagenesis. Asparagines N304, the Scw-specific N-glycosylation motif, and N342, the conserved N-glycosylation motif, were mutated into glutamine and named Scw^{N1Q} (N304Q), Scw^{N2Q} (N342Q) and Scw^{N1_N2Q} (N304Q and N342Q) (Fig. 2A). Wild-type or mutated Scw was expressed in *Drosophila* S2 cells,

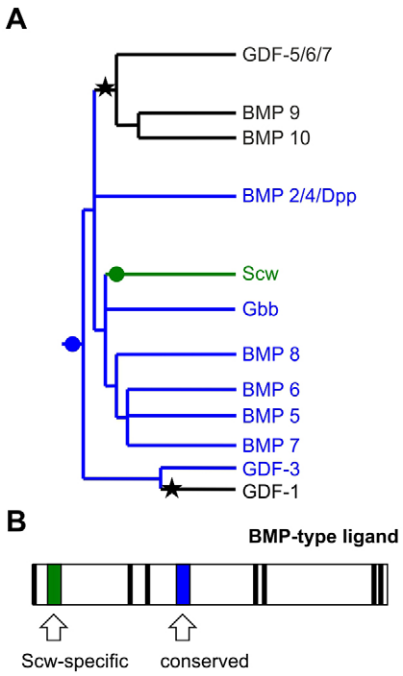

Fig. 1. N-glycosylation motifs in TGF-β-type ligand domains. (A) Schematic of the phylogenetic analysis of the TGF-β-type ligands (details in Fig. S1A). The phylogenetic tree includes BMP- and GDF-type ligands. The blue lines indicate the lineage of ligands that carry the BMP-type specific, conserved N-glycosylation motif. The green line represents the lineage with the Scw-specific N-glycosylation motif. Lineages with black lines have lost the conserved N-glycosylation motifs. Blue circle: gain of conserved N-glycosylation motif. Green circle: gain of Scw-specific N-glycosylation motif. Black asterisk: loss of N-glycosylation motifs. (B) Schematic figure of bioactive BMP-type ligands (sequence alignment in Fig. S1B). The BMP-type-specific N-glycosylation motif is shown in blue. The Scw-specific N-glycosylation motif is shown in green. Black bars indicate the positions of seven conserved cysteine residues within the ligand domain.

and their protein products were analyzed by western blotting. Scw^{WT} has a molecular mass of ∼15 kDa (Fig. 2B, lanes 1 and 4). Scw^{N1Q} and Scw^{N2Q} have an intermediate molecular mass of ∼13 kDa (Fig. 2B, lanes 5 and 6) and Scw^{N1_N2Q} appears to run at 10 kDa (Fig. 2B, lane 3). We treated Scw^{WT} with peptide-N-glycosidase (PNGase) F to elucidate whether secreted Scw^{WT} is indeed N-glycosylated. In fact, enzymatically deglycosylated Scw^{WT} revealed the same molecular mass as the secreted Scw N-glycosylation mutants (Scw^{N1_N2Q}) (Fig. 2B, lanes 2 and 3). These results indicate that both N-glycosylation motifs in the Scw ligand domains carry a carbohydrate moiety when they are expressed in S2 cells.

To understand how differentially glycosylated Scw ligands can form a heterodimer with Dpp, we performed comparative co-immunoprecipitation studies of Dpp with either wild-type or mutated Scw. All forms of the Scw ligand were able to heterodimerize with Dpp. After normalization, the relative amount of Dpp co-immunoprecipitated with Scw^{N1Q} and Scw^{N1_N2Q} is three-fold higher than that of Dpp:Scw^{WT} (Fig. 2C,D), suggesting that loss of the unique N-glycosylation motif of the Scw ligand facilitates Dpp:Scw heterodimer formation. Although the mechanisms behind preferential heterodimerization remain to be addressed, similar phenomena were observed when cleavage mutants of Scw were co-expressed with Dpp in S2 cells (Kunnapuu et al., 2014).

Next, we investigated the impact of N-glycosylation motifs on the signaling capacity of the Dpp:Scw heterodimer. We performed a

Development (2016) 143, 3742-3750 doi:10.1242/dev.130427

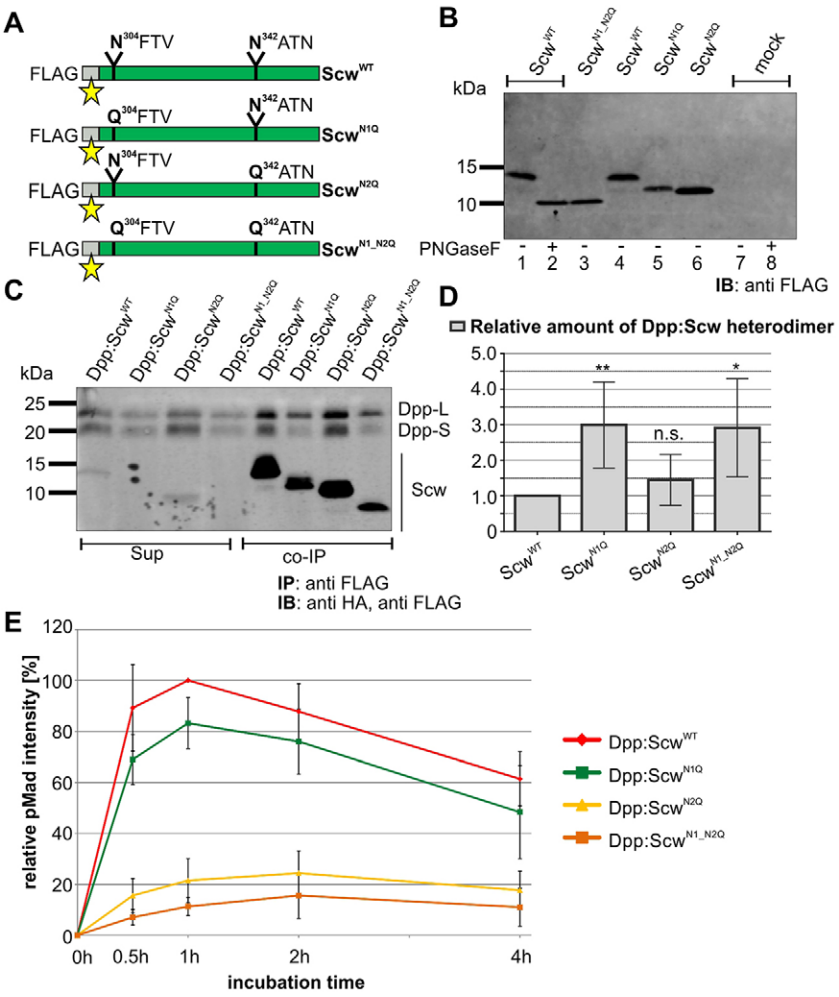

Fig. 2. N-glycosylation motifs in the Scw ligand domain impact BMP signaling *in vitro*. (A) Schematics of Scw^{WT}, Scw^{N1Q}, Scw^{N2Q} and Scw^{N1_N2Q} ligand domains. The N-glycosylation motifs are shown ($N^{304}FTV$ and $N^{342}ATN$). To elucidate whether both N-glycosylation motifs in the Scw ligand domain are utilized, the asparagine (N) was replaced by glutamine (Q). N1Q lacks the Scw-specific glycosylation motif (N304>Q304), N2Q lacks the conserved motif (N342>Q342) and N1_N2Q is the double mutant. The yellow asterisk indicates the position of a FLAG peptide. (B) Western blot analysis of the secreted Scw ligands described in A. Secreted proteins in supernatants were detected by probing with anti-FLAG antibody. Note that the molecular size of Scw^{WT} after PNGaseF treatment was identical to that of Scw^{N1_N2Q}. (C) Heterodimer formation of Dpp and wild-type or mutated Scw. Scw-FLAG (wild-type or glycosylation mutants) and Dpp-HA were expressed in S2 cells. Dpp-HA:Scw-FLAG heterodimers in conditioned medium (Sup) were purified using anti-FLAG M2 beads (co-IP) and Scw-FLAG and Dpp-HA detected by probing with anti-FLAG and anti-HA antibodies, respectively. Two different forms of Dpp (Dpp-S: 23 kDa and Dpp-L: 26 kDa) are detected (Kunnapuu et al., 2014). (D) The competence of Scw glycosylation mutants to form heterodimers with Dpp was analyzed by quantifying the relative amount of co-immunoprecipitated Dpp-HA (after normalization of precipitated Scw-FLAG) (number of experiments n=6, mean±95% CI; *P≤0.05, **P≤0.01, n.s., not significant, two-tailed Student's t-test). (E) Time course of relative BMP signaling in *Drosophila* S2 cells (based on data shown in Fig. S2). The pMad intensity in $Dpp:Scw^{WT}$ at 1 h of incubation is set to 100%. Mock data were set to 0%. Data are means±95% CI.

cell-based signaling assay (Kunnapuu et al., 2014): *Drosophila* S2 cells were incubated with equivalent amounts of either $Dpp:Scw^{WT}$, $Dpp:Scw^{N1Q}$, $Dpp:Scw^{N2Q}$ or $Dpp:Scw^{N1\_N2Q}$ heterodimers, and the signaling intensities were measured at different time points by quantifying the amount of phosphorylated Mad (pMad) in the cells as a direct readout of BMP signaling (Fig. S2A). A peak level signal of $Dpp:Scw^{WT}$ was achieved within the first hour of incubation (Fig. 2E) (Kunnapuu et al., 2014). The signaling of $Dpp:Scw^{N1Q}$, $Dpp:Scw^{N2Q}$ or $Dpp:Scw^{N1\_N2Q}$ was significantly weaker than that induced by $Dpp:Scw^{WT}$ within the first 2 hours of incubation (Fig. 2E, Fig. S2B). Loss of the conserved motif (Scw^{N2Q}) led to highly significant reduction of pMad signaling (Fig. S2B), whilst the effect of loss of the Scw-specific N-glycosylation motif (Scw^{N1Q}) on BMP signaling was less severe. Lack of two N-glycosylation motifs (Scw^{N1_N2Q}) caused an additive reduction of BMP signaling (Fig. 2E, Fig. S2B). Taken together, N-glycosylation of Scw ligand at two different positions contributes to maintain BMP signaling in S2 cells.

N-glycosylation motifs of the Scw ligand play crucial roles in fly viability

In order to understand how N-glycosylation of the Scw ligands is required for DV patterning in the *Drosophila* embryo, we first investigated the impact of N-glycosylation motifs of the Scw ligands on fly viability. The genomic rescue constructs containing the 4.8 kb *scw* locus *(g.scw)* (Kunnapuu et al., 2014) were mutated to $g.scw^{N1Q}$, $g.scw^{N2Q}$ or $g.scw^{N1\_N2Q}$ and inserted into the fly genome in a site-specific manner, using the PhiC31 integration system to avoid phenotypic variations due to differing insertion sites (Bischof et al., 2007). Wild-type *scw* ($g.scw^{WT}$) efficiently rescued *scw* null mutant flies [$scw^{S12}/Df(2L)OD16$] (1 copy: 90%; 2 copies: 145%). Flies carrying the $g.scw^{N1Q}$ construct showed a significantly reduced level of viability (1 copy: 40%; 2 copies: 88%). Flies lacking the conserved motif ($g.scw^{N2Q}$: 1 copy: 1%; 2 copies: 5%) or both motifs ($g.scw^{N1\_N2Q}$: 1 copy: 0%; 2 copies: 15%) were poorly rescued (Fig. 3A; Table S1). These results indicate that both N-glycosylation motifs are crucial for fully viable flies, although N1Q and N2Q mutations contribute to viabilities at different levels.

N-glycosylation motifs are needed for peak pMad level in the *Drosophila* early embryo

We then studied signaling of $g.scw^{WT}$, $g.scw^{N1Q}$, $g.scw^{N2Q}$ or $g.scw^{N1\_N2Q}$ in the blastoderm embryo. The analyzed embryos were at stage 5/6, chosen by onset of cephalic furrow formation. As a control, we analyzed pMad signaling in wild-type (*yw*) embryos (Fig. 3B, Fig. S3). Embryos with *scw* mutant background [$scw^{S12}/Df(2L)OD16$] do not show any detectable pMad signal (Fig. 3C, Fig. S3B). The pMad signals in the wild-type rescue flies [$scw^{S12}/Df(2L)OD16$; $g.scw^{WT}$/+] and rescued flies that lack the Scw-specific motif [$scw^{S12}/Df(2L)OD16$; $g.scw^{N1Q}$/+] were efficiently restored (Fig. 3D,E,H, Fig. S3B). The peak level of the pMad

Development (2016) 143, 3742-3750 doi:10.1242/dev.130427

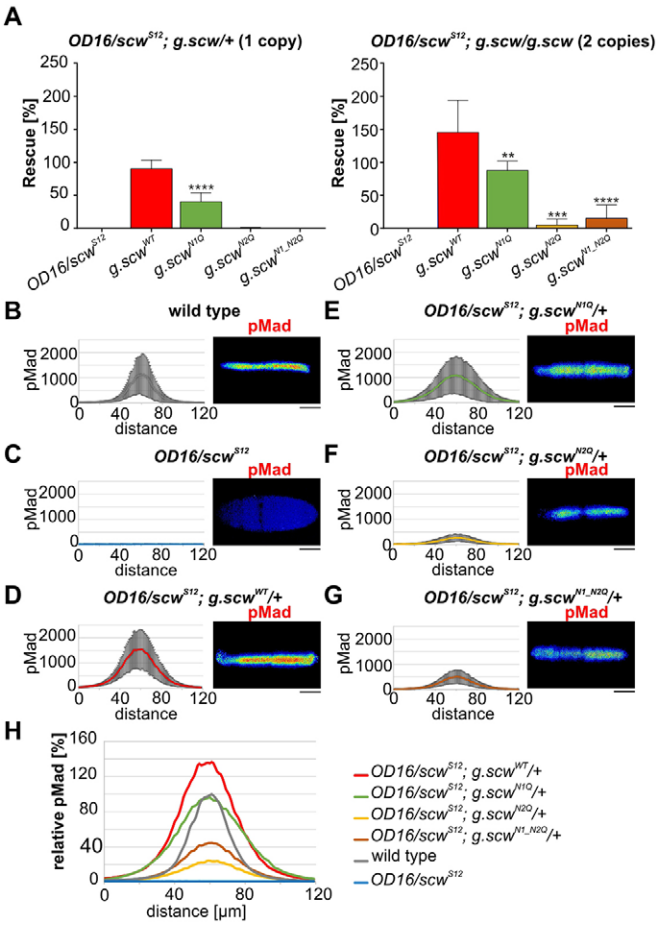

Fig. 3. N-glycosylation motifs in the Scw ligand domain are required for peak-level BMP signaling in the *Drosophila* early embryo. (A) $g.scw^{WT}$ constructs efficiently rescued *scw* null mutant flies [$Df(2L)OD16/scw^{S12}$] ($g.scw^{WT}$ 1 copy: 90%, 2 copies: 145%). Flies rescued with $g.scw^{N1Q}$ showed reduced viability ($g.scw^{N1Q}$ 1 copy: 40%, 2 copies: 88%). $g.scw^{N2Q}$ and $g.scw^{N1\_N2Q}$ constructs were not capable of efficiently rescuing *scw* null mutant flies ($g.scw^{N2Q}$ 1 copy: 1%, 2 copies: 5%; $g.scw^{N1\_N2Q}$ 1 copy: 0%, 2 copies: 15%). Graphs indicate means±95% CI, $^{**}P\leq0.01$, $^{***}P\leq0.005$, $^{****}P\leq0.0001$, Mann–Whitney *U*-test. (B-G) Mean intensity (left) and dorsal views of heat-mapped pMad staining (right) in stage 5/6 embryos. The anterior end is oriented to the left. Loss of N-glycosylation motifs in the Scw ligand domain leads to reduced BMP signaling. Wild-type embryos were analyzed as a control (B). Embryos of *scw* null mutant [$Df(2L)OD16/scw^{S12}$] do not show pMad signal (C). The mean intensity was calculated from five embryos per genotype (Fig. S3B). Error bars indicate s.d. Intensity is given in gray values. Mean intensity was plotted across 120 µm of the DV axis. Scale bars: 100 µm. (H) Comparison of relative pMad signaling of *scw* mutant flies expressing genomic rescue constructs. Peak level of the pMad signal in wild-type embryos was set to 100%.

signals in $scw^{S12}/Df(2L)OD16;\ g.scw^{WT}/+$ was higher than that of wild-type flies (Fig. 3H). The insertion position of the rescue construct may lead to increased expression of transformed genes. The average intensity of the pMad signals in $scw^{S12}/Df(2L)OD16;\ g.scw^{N1Q}/+$ was lower than that in flies carrying the scw^{WT} rescue construct (Fig. 3H). In contrast, consistent with the cell-based signaling assay, loss of the conserved motif ($scw^{S12}/Df(2L)OD16;\ g.scw^{N2Q}/+$) or both motifs [$scw^{S12}/Df(2L)OD16;\ g.scw^{N1\_N2Q}/+$] resulted in lower pMad signals than that in wild-type embryos (Fig. 3F-H, Fig. S3B). These results indicate that both N-glycosylation motifs in the Scw ligand domain are needed for peak level signaling in the early embryo.

Signaling of N-glycosylation-modified Gbb and Scw ligands in the embryo and pupal wing

scw can rescue *gbb* mutants in the context of PCV formation in a non-reciprocal manner (Fritsch et al., 2010; Matsuda and Shimmi, 2012). It is not clear whether structural changes of ligands lead to context-specific properties, or whether ligands are differentially produced or secreted. We wondered whether the Scw ligand acquiring a unique N-glycosylation motif could represent a crucial change facilitating its context specific activity, or if the Scw prodomain contributes to production or secretion of ligands in the embryo. To address these issues, we introduced an N-glycosylation motif into the Gbb ligand domain at the corresponding position of the Scw-specific N-glycosylation motif and generated chimeric proteins consisting of Scw prodomain and Gbb ligand domain, either with (Scw-Gbb^{+Glc}) or without (Scw-Gbb^{WT}) the additional N-glycosylation motif (Fig. 4A). These chimeric proteins are expressed in *Drosophila* S2 cells. Co-immunoprecipitation experiments revealed that Scw-Gbb^{WT} and Scw-Gbb^{+Glc} are secreted and capable of heterodimer formation with Dpp in S2 cells (Fig. 4B). We then elucidated the functionality of Scw-Gbb chimeras *in vivo*. We obtained transgenic animals carrying UAS constructs containing various ligand cDNAs by using the same genomic insertion site (Bischof et al., 2007). To study BMP signaling in the blastoderm embryo, genes under the control of UAS enhancer were overexpressed at the anterior part of the embryo with a *bicoid* (*bcd*)-*Gal4* driver (Fig. 4C) (Shimmi et al., 2005b). Overexpression of wild-type or mutated Scw restored the pMad signal in the anterior part of *scw* mutant embryos (Fig. 4C). Intriguingly, pMad signal was only restored in the cells where Gal4 is active. Laterally expressed Sog appears to redistribute Scw for peak level signal induction. These observations are consistent with an idea that the *sog* expression pattern instructs the positional information of signaling, but not the ligand expression pattern. In contrast, we did not observe any detectable pMad signal in *scw* null mutant embryos overexpressing Scw-Gbb^{WT} or Scw-Gbb^{+Glc}, suggesting that Gbb ligands are intrinsically unable to transduce signal in *Drosophila* embryos.

To test whether these ligands are functional in different developmental contexts, we assessed PCV formation in the pupal wing. pMad signal regulated by the BMP network is an initial cue for PCV development during the pupal stage. Previous work showed that either *gbb* or *scw*, expressed with the dpp^{shv} driver, could restore pMad signaling in the PCV region of *gbb* mutants (Matsuda and Shimmi, 2012). Expression of wild-type *scw*, mutated *scw* or *scw-gbb* chimera led to rescue of pMad signaling during PCV development (Fig. 4D). Hence, the chimeric protein Scw prodomain-Gbb ligand is functional *in vivo*. We observed that pMad signaling in the PCV region was highly variable among individuals when wild-type or mutated *scw* or *scw-gbb* was expressed, thus it was challenging to quantify pMad signaling in the pupal wing due to technical difficulties. Since PCV formation in the adult wing can be used as a marker of BMP signal induction during PCV development, we performed screening of adult wings for PCV formation and investigated the capabilities of these ligands to restore PCV formation in a crossveinless *gbb* mutant background ($gbb^{51}/gbb^{4};\ dpp^{shv}$-*Gal4*) (Fig. 5). As previously reported (Matsuda and Shimmi, 2012), Scw^{WT} restored the PCV formation, but with some variability: 60% rescued, 17% partially rescued (Fig. 5B). Expression of scw^{N1Q}, scw^{N2Q}, or scw^{N1_N2Q} rescued with different efficiencies (Scw^{N1Q}: 87% rescued; Scw^{N2Q}: 64% rescued, 19% partially rescued; Scw^{N1Q_2Q}: 100% rescued) (Fig. 5C-E). Constructs carrying the chimeric Scw-Gbb with or without additional N-glycosylation motif also showed

Development (2016) 143, 3742-3750 doi:10.1242/dev.130427

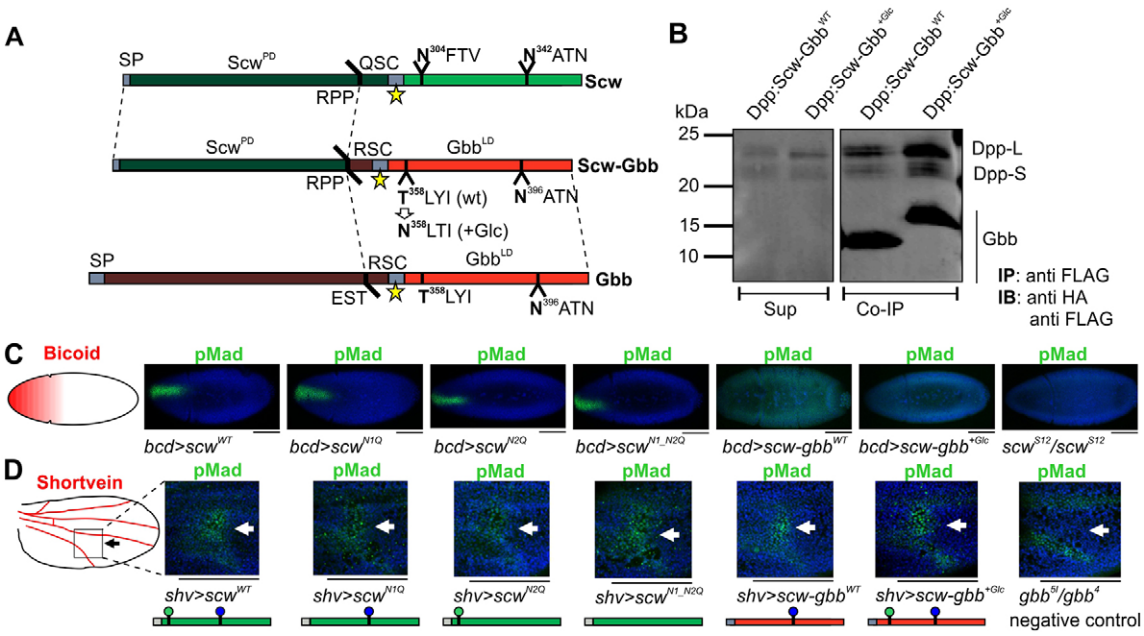

Fig. 4. Scw and Gbb show distinct functions in the early embryo and the PCV formation during pupal stage. (A) Schematic of the generation of a Scw-Gbb chimera constructed by fusing the Scw prodomain (Scw^{PD}) with the Gbb ligand domain (Gbb^{LD}). Chimeras of both Gbb^{WT}, carrying single N-glycosylation motif ($N^{396}ATN$) and Gbb^{+Glc}, carrying a second N-glycosylation motif ($T^{358}LYI>N^{358}LTI$), were generated. SP indicates the N-terminal signal peptide. The yellow asterisk indicates the position of a FLAG peptide. (B) Heterodimer formation of Dpp and Scw-Gbb chimeras. Scw-Gbb-FLAG (wild-type or +glycosylation motif) and Dpp-HA were expressed in *Drosophila* S2 cells. Dpp-HA:Scw-Gbb-FLAG heterodimers in conditioned medium were purified through anti-FLAG M2 beads (Co-IP). Scw-Gbb-FLAG and Dpp-HA were detected by probing with anti-FLAG and anti-HA antibodies. These results indicate that Scw-Gbb chimeras are secreted and capable of heterodimerization with Dpp. Blots of supernatant (Sup) and Co-IP were derived from the same membrane. (C,D) Illustrations show the expression pattern of the *bicoid* (*bcd*)-*Gal4* driver in the early embryo (C) and the *shortvein* (dpp^{shv})-*Gal4* driver in the pupal wing (D), respectively. (C) Dorsal view of pMad (green) and DAPI (nuclear marker, blue) staining in the early embryo (stage 5/6) expressing wild-type or mutated *scw*, $scw\text{-}gbb^{WT}$ or $scw\text{-}gbb^{+Glc}$ with *bcd-Gal4* in *scw* null (scw^{S12}/scw^{S12}) mutants. Expression of scw^{WT}, scw^{N1Q}, scw^{N2Q}, or scw^{N1_N2Q} results in pMad signal in the anterior part of the early embryo. Neither $Scw\text{-}Gbb^{WT}$ nor $Scw\text{-}Gbb^{+Glc}$ chimeras were able to induce pMad signal in the early embryo. No pMad signal is observed in the *scw* mutant embryos. The anterior end of the embryos is oriented to the left. (D) PCV region of pupal wings. pMad (green) and DAPI (blue) staining in pupal wings at 24 h after pupariation. Scw and Gbb can induce pMad signal in the pupal wing. Expression of *scw* (wild-type or N-glycosylation mutants), $scw\text{-}gbb^{WT}$ or $scw\text{-}gbb^{+Glc}$ driven by dpp^{shv}-*Gal4* in *gbb* mutant flies (gbb^{5l}/gbb^{4}) enables PCV development presumably through induction of long-range BMP signaling into PCV regions. The PCV position is indicated by arrows. Blue circle: conserved N-glycosylation motif; green circle: Scw-specific N-glycosylation motif. Scale bars: 100 µm.

different efficiency in restoring the PCV ($Scw\text{-}Gbb^{WT}$: 86% rescued, 1% partially rescued; $Scw\text{-}Gbb^{+Glc}$: 28% rescued, 49% partially rescued) (Fig. 5F,G). Thus, the order of fully rescued PCV formation is as follows: Scw^{N1_N2Q}>$Scw\text{-}Gbb^{WT}$=Scw^{N1Q}>Scw^{WT}=Scw^{N2Q}>$Scw\text{-}Gbb^{+Glc}$. Based on these results, we conclude that the $scw\text{-}gbb^{+Glc}$ chimeric proteins are functional in the context of PCV formation. It is noteworthy, however, that the Scw-specific N-glycosylation motif does not provide a benefit during PCV formation, instead, it decreases the developmental reproducibility.

N-glycosylation of Scw ligand domain facilitates ligand secretion

To further address how Scw mutants are utilized through ligand production and secretion, we investigated ligand localization when *scw* mutants were expressed in larval wing imaginal discs. A co-localization study of *Scw* glycosylation mutants and the endoplasmic reticulum (ER) reveals that Scw^{WT}, Scw^{N1Q} and Scw^{N2Q} correlate with the ER to a comparable extent. In contrast, Scw^{N1_N2Q} shows increased colocalization with the ER (Fig. S4). These data suggest that the N-glycosylation motif may facilitate Scw ligand secretion.

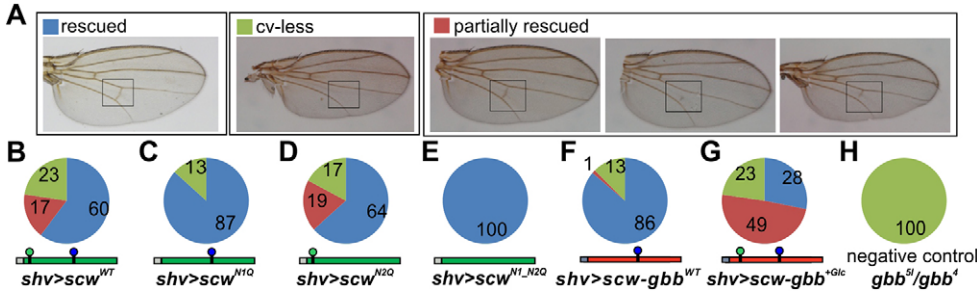

Fig. 5. N-glycosylation of BMP ligands reduces their functionality in PCV development. (A) Phenotypes of PCV development in adult wings. A rescued wing reflects the wild-type phenotype. (B-H) Ratios of fully rescued, partially rescued or crossvein (cv)-less phenotypes. Number of counted wings: $shv>scw^{WT}$: 53; $shv>scw^{N1Q}$: 105; $shv>scw^{N2Q}$: 93; $shv>scw^{N1\_N2Q}$: 56; $shv>scw\text{-}gbb^{WT}$: 80; $shv>scw\text{-}gbb^{+Glc}$: 110; gbb^{4}/gbb^{5l}: 63. Note that less-glycosylated ligands restore crossveinless phenotypes more efficiently. Blue circle: conserved N-glycosylation motif; green circle: Scw-specific N-glycosylation motif.

Development (2016) 143, 3742-3750 doi:10.1242/dev.130427

To confirm this finding, we quantitatively analyzed Scw ligand production and secretion in S2 cells. Wild-type or mutated Scw was expressed in *Drosophila* S2 cells and the protein products in cell lysates and supernatants were measured by western blotting. Equivalent protein levels of Scw^{WT}, Scw^{N1Q} and Scw^{N2Q} in both cell lysates and supernatants were observed (Fig. 6). In contrast, although the Scw^{N1_N2Q} protein was sufficiently produced in cell lysates, its levels in supernatants were significantly lower than those of Scw^{WT}, Scw^{N1Q} or Scw^{N2Q} (Fig. 6, bottom panel). These results further indicate that the N-glycosylation sites of Scw consistently facilitate Scw ligand secretion.

DISCUSSION

This study provides insights into how evolutionary and developmental pressures shape molecules after their divergence from a common ancestor. We show that a conserved N-glycosylation motif exists, which is specific for BMP-type ligands throughout various animal species. In addition, we observed that the BMP5-8-type ligand Scw contains a unique N-glycosylation motif that helps to maintain a peak level of BMP signal in the embryo. In contrast, N-glycosylation modifications of BMP-type ligands reduce the consistency in PCV development. Our observations provide insights into how evolutionarily conserved signaling molecules adapt to developmental processes.

N-glycosylation of BMP-type ligands in developmental processes

The significance of N-glycosylation of the TGF-β-type ligands has been studied previously. For example, N-glycosylation of the BMP2 prodomain affects the folding and secretion of ligands, and non-glycosylated BMP2 and BMP6 produced in bacterial cells appear to be less active than the glycosylated ligands (Schmoekel et al., 2004; Saremba et al., 2008; van de Watering et al., 2012; Hang et al., 2014). Addition of an N-glycosylation motif in Nodal changes the stability of ligands, resulting in an increased signaling range (Le Good et al., 2005). These facts suggest that N-glycosylation of ligands may play significant roles *in vivo*. However, these roles have been largely unexplored because of a lack of *in vivo* model systems. By employing both *in vivo* studies and cell-based experiments, we investigated how N-glycosylation modifications of the BMP-type ligands impact developmental processes. The *in vivo* rescue experiments revealed that these motifs are crucial for fly viability and are required to achieve peak level BMP signaling. Loss of the Scw-specific motif leads to a reduced impact on BMP signaling in the embryo compared with the effect of the conserved motif but also to less signaling capacity when compared to Scw^{WT}, resulting in lower viability of $g.scw^{N1Q}$ rescued flies (Fig. 3A). On the other hand, integration of the Scw-specific N-glycosylation motif into its paralog Gbb (Scw-Gbb chimera) is not sufficient to provide functionality in the early embryo (Fig. 4). This suggests that the critical changes responsible for the differing specificity of the Gbb and Scw ligands that developed after gene duplication may be differences in the primary sequences other than N-glycosylation motifs.

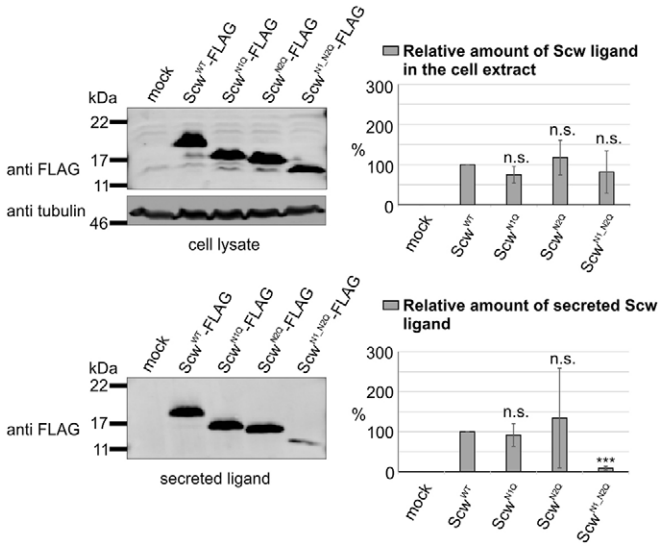

Fig. 6. N-glycosylation motif of Scw ligands facilitates ligand secretion in S2 cells. Western blot analysis of *Drosophila* S2 cell lysate and supernatant. Cells were either mock transfected or transfected with *UAS-scw^{WT}*, *UAS-scw^{N1Q}*, *UAS-scw^{N2Q}* and *UAS-scw^{N1_N2Q}*, respectively. The upper panel shows the expression level of Scw^{WT} and Scw glycosylation mutants in the cell extract. Tubulin acts as an internal control. The lower panel shows the expression level in the supernatant. The graphs illustrate mean±s.d. of relative expression levels. Scw^{N1Q}, Scw^{N2Q} and Scw^{N1_N2Q} expression levels were normalized towards Scw^{WT}. Note that Scw^{WT}, Scw^{N1Q} and Scw^{N2Q} appear to be equally secreted. In contrast, the amount of secreted Scw^{N1_N2Q} compared with Scw^{WT} is significantly reduced, indicating that Scw^{N1_N2Q}, but not Scw^{N1Q} and Scw^{N2Q}, is either less efficiently secreted or less stable. The significance was calculated from five independent experiments (n=5). Each experiment consists of two technical replicates. The average of the technical replicates was used to calculate the mean and the standard deviation of the five independent experiments. (***P≤0.001, n.s., not significant; two-tailed Student's t-test).

As reported in the case of Nodal (Le Good et al., 2005), adding N-glycosylation sites to ligands may change protein stability/secretion and therefore may affect *in vivo* phenotypes. In the case of Scw, we presume that acquisition of the unique N-glycosylation motif has no drastic effect on protein stability/secretion, but instead directly affects the signaling outcome. First, equal amounts of differentially glycosylated ligands show different signaling intensities in the cell-based assay (Fig. 2). Second, expression of differentially glycosylated ligands showed different signaling intensities in the embryo when they are expressed in identical genetic backgrounds (Fig. 3). Third, the total protein levels in both cell lysates and supernatants for Scw^{WT}, Scw^{N1Q} and Scw^{N2Q} are equivalent when they are expressed in S2 cells (Fig. 6). Thus, these results suggest that changing the number and positions of N-glycosylation motifs may impact signaling intensities both *in vivo* and *in vitro* without significantly changing protein stability/secretion. In contrast, non-glycosylated Scw ligand (Scw^{N1_N2Q}) appears to be less efficiently secreted (Fig. 6). These facts suggest that at least one N-glycosylation site of Scw is crucial for maintaining protein stability/secretion, but their number or position may not be essential for secretion (Guerriero and Brodsky, 2012).

Interestingly, N-glycosylation of the ligands did not provide any advantage for PCV formation. Instead, the Scw ligand lacking both N-glycosylation motifs (Scw^{N1_N2Q}) most efficiently restored the PCV-less phenotypes in *gbb* mutant wings (Fig. 5). We hypothesize that N-glycosylation of BMP ligands does not always benefit extracellular trafficking of ligands. Highly glycosylated ligands may interact with enriched extracellular matrix (ECM) at the basal side of wing epithelia and reduce the ligand mobility regulated by the BMP network (Fristrom et al., 1993). Alternatively, differential expression of key molecules may explain different phenotypes between embryogenesis and crossvein development. It has been previously reported that the heparan sulfate proteoglycan (HSPG) Dally impacts BMP signaling in various contexts. Dally plays a role in Dpp gradient formation in the wing imaginal disc by stabilizing Dpp (Akiyama et al., 2008; Dejima et al., 2011) and it increases the signaling of Gbb and Dpp in *Drosophila* S2 cells (Dejima et al.,

Development (2016) 143, 3742-3750 doi:10.1242/dev.130427

2011). In addition, lack of Dally and Dally-like protein (Dlp) affects PCV formation in the wing (Serpe et al., 2008; Chen et al., 2012). Interestingly, HSPGs are absent within the first 3 hours of embryogenesis (Bornemann et al., 2008), which is the only time frame of *scw* expression (Arora et al., 1994). Based on these facts, it appears that Scw and HSPGs are mutually exclusive. This may partly explain why non-glycosylated Scw is functional for PCV development but not for embryonic DV patterning. Furthermore, the Scw^{N1_N2Q}:Dpp heterodimer is likely to be a primary ligand responsible for BMP signaling in the PCV region. Since Dpp carries the conserved N-glycosylation motif, the Scw^{N1_N2Q}:Dpp heterodimer contains one N-glycosylation site, although Scw^{N1_N2Q} lacks N-glycosylation site. The N-glycosylation site of Dpp may help facilitate Scw^{N1_N2Q}:Dpp heterodimer secretion.

Why is a unique N-glycosylation site acquired in the Scw ligand? *scw* is exclusively expressed in the early embryo (Arora et al., 1994; FlyBase, 2012), which is in contrast to the usually recurrent activity of signaling molecules at different stages of development. The model we favor is that random mutations create differential N-glycosylation motifs in otherwise functionally redundant and conserved ligands. These novel motifs lead to structural changes that confer either advantages or disadvantages, depending on the developmental context. Since a positive feedback mechanism is crucial for DV patterning in *Drosophila* (Wang and Ferguson, 2005), acquisition of the unique N-glycosylation site could bring an advantage to Scw signaling. In contrast, in a wide range of species including humans, BMP2/4- and BMP5-8-type ligands are repeatedly utilized for development at different stages and in different positions. Therefore, to provide robustness and reproducibility in various contexts, vertebrate BMP2/4 and BMP5-8 contain only one N-glycosylation site to impose developmental constraints: stronger signaling than a non-glycosylated ligand, and less impeded extracellular trafficking than additionally glycosylated ligands. Consistently, Gbb has been shown to function at various developmental stages (Khalsa et al., 1998; McCabe et al., 2003; Kawase et al., 2004; Ballard et al., 2010).

Evolutionary aspects

Although various co-factors of the BMP network have been identified among species, it remains to be addressed how they adapted to different developmental stages and different species. The *scw* allele was originally identified as a DV patterning defect (Nusslein-Volhard, 1984) and was determined to encode a BMP5-8-type protein (Arora et al., 1994). It was then proposed that *scw* originates from gene duplication of *gbb* in the branch leading to higher Diptera (Van der Zee et al., 2008; Fritsch et al., 2010), a highly diverged branch in the arthropod lineage (Wotton et al., 2013; Misof et al., 2014). Hence, *gbb* and *scw* provide an outstanding opportunity to investigate evolutionary divergence of protein structures. In *Drosophila*, *gbb* and *scw* are expressed in distinct patterns, but both function as co-factors of the BMP network. A recent study indicates both Gbb and Scw are utilized for DV patterning in the scuttle fly (Rafiqi et al., 2012). *gbb* expression was also described in the early embryo of the lower Dipteran *Clogmia albipunctata*, in which the *scw* gene was not found (Wotton et al., 2013). These facts indicate a possibility that Gbb acts as a co-factor of the BMP network for DV patterning in most arthropod species and that Scw evolved specifically for DV patterning in higher Diptera after duplication of the *scw*-like gene *gbb*. Further studies are needed to elucidate how Gbb lost the capacity to transduce signals in the *Drosophila* blastoderm embryo.

In summary, our data reveal that two BMP5-8-type ligands, Scw and Gbb, which function as co-factors of the BMP network, provide a unique model to investigate how orthologous proteins evolve under developmental and evolutionary constraints. Further studies in this context will help elucidate how evolutionarily conserved molecules generate diversified structures in the animal kingdom.

MATERIALS AND METHODS

DNA constructs

scw-Flag, *dpp-HA* and *gbb-Flag* for cell culture experiments were described previously (Shimmi et al., 2005a,b; Kunnapuu et al., 2009). To generate scw^{N1Q}, scw^{N2Q}, scw^{N1_N2Q} and gbb^{+Glc} mutants, the QuikChange II Site-Directed Mutagenesis Kit (Agilent Technologies) was used. Generation of the genomic *scw* (*g.scw*) construct was described previously (Kunnapuu et al., 2014). To simplify mutagenesis and subcloning steps, the 2086 bp scw *Cla*I fragment was inserted into pBluescriptKS(+) [pBS.g.scw (piece)]. A part of the *scw* coding sequence containing the FLAG-tag was subcloned into pBS.gscw (piece), using *Nde*I and *Bal*I restriction sites. The glycosylation sites were mutated by using the QuikChange II Site-Directed Mutagenesis Kit. As an intermediate step, the *g.scw* (*piece*) fragments were subcloned into pCR-Blunt IITOPO vector (Life Technologies) containing the 4.8 kb genomic *scw* fragment described previously (Kunnapuu et al., 2014) by using *Cla*I restriction sites. The resulting 4.8 kb genomic wild-type or mutated *scw* fragments were subcloned into the *pattB* vector. For scw^{PD}-gbb^{LD} chimeric constructs, we used overlap extension (OE) PCR. To fuse scw^{PD} and gbb^{LD} seamlessly, the following OE primers were used: scw.gbbOE fw 5′**ACGACGACAA-GCAGTCC**TGCCAGATGCAGACCCT3′ and scw.gbbOE rev 5′AGG-GTCTGCATCTGGCA**GGACTGCTTGTCGTCGT**3′.

Bold characters indicate the *scw* region, others cover the *gbb* domain. For the *UAS.scw* and *UAS.*scw^{PD}-gbb^{LD} constructs, the coding sequences were subcloned into pUASg.attB vector.

Drosophila stocks

Df(2L)OD16, *bicoid-Gal4*, dpp^{shv}-*Gal4*, gbb^{4}, gbb^{51} and scw^{S12} were described previously (Shimmi et al., 2005b; Matsuda and Shimmi, 2012; Kunnapuu et al., 2014). *apterous-Gal4* was obtained from Bloomington *Drosophila* Stock Center (#3041). *pUASg.attB.scw*, *pUASg.attB.*scw^{PD}.gbb^{LD} and *pattB.g.scw* constructs were inserted into the fly genome at chromosomal position 86Fb on chromosome III in a site-specific manner, using the PhiC31 integration system (Bischof et al., 2007).

Rescue experiment with transgenic flies

For the rescue experiment with one copy of the genomic rescue construct, scw^{S12}*/CyO, g.scw/g.scw* transgenic flies were crossed to *Df(2L)OD16/CyO*. For the rescue experiment with two copies of the genomic rescue construct, scw^{S12}*/CyO, g.scw/g.scw* transgenic flies were crossed to *Df(2L)OD16/CyO; g.scw/g.scw*. For the negative control, scw^{S12}*/CyO* flies were crossed to *Df(2L)OD16/CyO*. The exact number of crosses and fly genotypes can be found in Table S1. Twenty crosses (1 virgin female/cross) were set up for each genotype. To calculate the survival rate of each single cross, half of the number of *CyO* progeny [which were either scw^{S12}/*CyO* or *Df(2L)OD16/CyO*] was considered as 100%. Non-*CyO* progeny were considered to have *scw* mutant background [*Df(2L)OD16/*scw^{S12}]. Statistics were performed by GraphPad Prism for Windows.

Immunostaining of *Drosophila* embryos, pupal wings and wing imaginal disc

Embryo collection and staining were described previously (Kunnapuu et al., 2014). The fixed tissues were stained with phospho-Smad1/5 rabbit monoclonal antibody (anti-pMad) at 1:1000 (#9516, Cell Signaling Technology) as a primary antibody and TSA Plus Fluorescein System (PerkinElmer) to visualize the fluorescence images. Lack of *lacZ* expression in *CyO, wg-lacZ* or *CyO, ftz-lacZ* and presence of *lacZ* in *Df(2L)OD16, kr-lacZ* was used to identify homozygous *scw* mutants. *yw* flies were used as wild-type strains. For quantification of pMad signal, we followed the protocol described previously (Gavin-Smyth et al., 2013). The embryos

Development (2016) 143, 3742-3750 doi:10.1242/dev.130427

were stained and imaged on the same day under identical conditions. The pMad intensity of a 32-bit SUM *z*-stack projection was measured within a 120×200 µm rectangle. The rectangle was centered at the pMad and the *kr-lacZ* stripe (see also Fig. S3).

Pupal wings were dissected 24 h after pupariation and fixed at 4°C overnight in 3.7% formaldehyde. The fixed tissues were stained with anti-pMad at 1:1000 (#9516, Cell Signaling Technology) as a primary antibody and anti-rabbit IgG Alexa Fluor 568 at 1:200 (#A11011, Thermo Fisher Scientific) as a secondary antibody. Lack of GFP expression in *CyO, act-GFP* was used to identify homozygous mutant flies.

Wing imaginal discs were dissected from third instar larvae and fixed for 30 min in 3.7% formaldehyde. Scw-FLAG was visualized with mouse anti-FLAG at 1:300 (#F1804, Sigma), the ER was visualized with rat anti-KDEL at 1:400 (#ab50601, Abcam), and the cell membrane was stained with rabbit-anti-Scribble [obtained from Chris Doe (Albertson et al., 2004)]. Secondary antibodies were used at 1:200: Alexa Fluor 488 goat anti-rat (#A11006, Thermo Fisher), Alexa Fluor 647 goat anti-rabbit (#A21244, Thermo Fisher), Alexa Fluor 568 goat anti-mouse (#A11004, Thermo Fisher). The wing imaginal discs were stained and imaged on the same day under identical conditions. Fluorescence images were obtained with a Zeiss LSM 700. Image analysis was performed with ImageJ. Statistical tests were carried out using Microsoft Excel.

Correlation study of Scw-FLAG glycosylation mutants and the ER in the wing imaginal disc

Correlation of the red (Scw-FLAG) and the green channel (KDEL) was analyzed with Imaris software (BitPlane). For calculation of the Pearson's coefficient, the threshold for both channels was set to 10% of the respective maximum intensity.

Recombinant proteins and cell culture experiments

UAS.dpp^{WT}-HA, *UAS.scw^{WT}-FLAG*, *UAS.scw^{N1Q}-FLAG*, *UAS.scw^{N2Q}-FLAG*, *UAS.scw^{N1_N2Q}-FLAG*, *UAS.scw-gbb^{WT}-FLAG* or *UAS.scw-gbb^{+Glc}-FLAG* was co-transfected with *tubulin-Gal4* for protein expression in *Drosophila* S2 cells. Dpp:Scw co-immunoprecipitation was performed as described previously (Kunnapuu et al., 2014).

To elucidate the N-glycosylation state of the Scw or Scw-Gbb chimera, either S2 cell supernatant or cell lysate was treated with PNGaseF (New England Biolabs) for 8 h at 37°C. Antibodies and western blot analysis were as described (Kunnapuu et al., 2014).

The BMP signaling assay was performed as previously described (Kunnapuu et al., 2014). Mouse-anti-tubulin (#T6199, Sigma) was used at 1:5000 as an internal control. The signaling intensity was measured by probing western blots with rabbit anti-pMad at 1:2000 (a gift from Peter ten Dijke, Leiden University, The Netherlands) followed by incubation with secondary antibodies: anti-mouse IRDye 680LT 1:4000 (#926-68020, Li-COR) and anti-rabbit IRDye 800CW 1:2000 (#926-32211, Li-COR). Western blots were analyzed using the Odyssey Infrared Imaging System (LI-COR). Signal intensities were quantified by using Odyssey Imaging Software (LI-COR). Statistical analyses were performed in MS Excel and GraphPad Prism for Windows.

Phylogenetic analysis

Multiple sequence alignments were performed by using Clustal Omega (Goujon et al., 2010; Sievers et al., 2011). Sequence alignments were analyzed by using GeneDoc software and MEGA6. Phylogenetic analyses were conducted in MEGA6 (Tamura et al., 2013).

Acknowledgements

We thank Martin Kracklauer and Daniel Toddie-Moore for thoughtful comments on the manuscript. We are grateful to Jaana Vulli for her support in the initial phase of the project. We also thank Ari Löytynoja for consultation about phylogenetic analysis.

Competing interests

The authors declare no competing or financial interests.

Author contributions

P.M.T. performed most of the experiments and all data analysis. J.G. performed wing experiments. P.M.T. and O.S. designed the experiments and wrote the paper.

Funding

This work was supported by the Academy of Finland (Suomen Akatemia) [265648 to O.S. and Center of Excellence in Experimental and Computational Developmental Biology]; the Sigrid Juselius Foundation (O.S.); and the Integrative Life Science Doctoral Program of the University of Helsinki (J.G.).

Supplementary information

Supplementary information available online at
http://dev.biologists.org/lookup/doi/10.1242/dev.130427.supplemental

References

Abzhanov, A., Protas, M., Grant, B. R., Grant, P. R. and Tabin, C. J. (2004). Bmp4 and morphological variation of beaks in Darwin's finches. *Science* **305**, 1462-1465.

Akiyama, T., Kamimura, K., Firkus, C., Takeo, S., Shimmi, O. and Nakato, H. (2008). Dally regulates Dpp morphogen gradient formation by stabilizing Dpp on the cell surface. *Dev. Biol.* **313**, 408-419.

Albertson, R., Chabu, C., Sheehan, A. and Doe, C. Q. (2004). Scribble protein domain mapping reveals a multistep localization mechanism and domains necessary for establishing cortical polarity. *J. Cell Sci.* **117**, 6061-6070.

Arora, K., Levine, M. S. and O'Connor, M. B. (1994). The screw gene encodes a ubiquitously expressed member of the TGF-beta family required for specification of dorsal cell fates in the Drosophila embryo. *Genes Dev.* **8**, 2588-2601.

Ballard, S. L., Jarolimova, J. and Wharton, K. A. (2010). Gbb/BMP signaling is required to maintain energy homeostasis in Drosophila. *Dev. Biol.* **337**, 375-385.

Bier, E. and De Robertis, E. M. (2015). Embryo development. BMP gradients: a paradigm for morphogen-mediated developmental patterning. *Science* **348**, aaa5838.

Bischof, J., Maeda, R. K., Hediger, M., Karch, F. and Basler, K. (2007). An optimized transgenesis system for Drosophila using germ-line-specific phiC31 integrases. *Proc. Natl. Acad. Sci. USA* **104**, 3312-3317.

Bornemann, D. J., Park, S., Phin, S. and Warrior, R. (2008). A translational block to HSPG synthesis permits BMP signaling in the early Drosophila embryo. *Development* **135**, 1039-1047.

Carroll, S. B. (2008). Evo-devo and an expanding evolutionary synthesis: a genetic theory of morphological evolution. *Cell* **134**, 25-36.

Chen, J., Honeyager, S. M., Schleede, J., Avanesov, A., Laughon, A. and Blair, S. S. (2012). Crossveinless d is a vitellogenin-like lipoprotein that binds BMPs and HSPGs, and is required for normal BMP signaling in the Drosophila wing. *Development* **139**, 2170-2176.

Dejima, K., Kanai, M. I., Akiyama, T., Levings, D. C. and Nakato, H. (2011). Novel contact-dependent bone morphogenetic protein (BMP) signaling mediated by heparan sulfate proteoglycans. *J. Biol. Chem.* **286**, 17103-17111.

De Robertis, E. M. (2008). Evo-devo: variations on ancestral themes. *Cell* **132**, 185-195.

De Robertis, E. M. and Sasai, Y. (1996). A common plan for dorsoventral patterning in Bilateria. *Nature* **380**, 37-40.

Dickinson, D. J., Weis, W. I. and Nelson, W. J. (2011). Protein evolution in cell and tissue development: going beyond sequence and transcriptional analysis. *Dev. Cell* **21**, 32-34.

Fristrom, D., Wilcox, M. and Fristrom, J. (1993). The distribution of PS integrins, laminin A and F-actin during key stages in Drosophila wing development. *Development* **117**, 509-523.

Fritsch, C., Lanfear, R. and Ray, R. P. (2010). Rapid evolution of a novel signalling mechanism by concerted duplication and divergence of a BMP ligand and its extracellular modulators. *Dev. Genes Evol.* **220**, 235-250.

Gavin-Smyth, J., Wang, Y.-C., Butler, I. and Ferguson, E. L. (2013). A genetic network conferring canalization to a bistable patterning system in Drosophila. *Curr. Biol.* **23**, 2296-2302.

Genikhovich, G., Fried, P., Prunster, M. M., Schinko, J. B., Gilles, A. F., Fredman, D., Meier, K., Iber, D. and Technau, U. (2015). Axis patterning by BMPs: cnidarian network reveals evolutionary constraints. *Cell Rep.* **10**, 1646-1654.

Goltsev, Y., Fuse, N., Frasch, M., Zinzen, R. P., Lanzaro, G. and Levine, M. (2007). Evolution of the dorsal-ventral patterning network in the mosquito, Anopheles gambiae. *Development* **134**, 2415-2424.

Goujon, M., McWilliam, H., Li, W., Valentin, F., Squizzato, S., Paern, J. and Lopez, R. (2010). A new bioinformatics analysis tools framework at EMBL-EBI. *Nucleic Acids Res.* **38**, W695-W699.

Guerriero, C. J. and Brodsky, J. L. (2012). The delicate balance between secreted protein folding and endoplasmic reticulum-associated degradation in human physiology. *Physiol. Rev.* **92**, 537-576.

Hang, Q., Zhou, Y., Hou, S., Zhang, D., Yang, X., Chen, J., Ben, Z., Cheng, C. and Shen, A. (2014). Asparagine-linked glycosylation of bone morphogenetic protein-2 is required for secretion and osteoblast differentiation. *Glycobiology* **24**, 292-304.

Kawase, E., Wong, M. D., Ding, B. C. and Xie, T. (2004). Gbb/Bmp signaling is essential for maintaining germline stem cells and for repressing bam transcription in the Drosophila testis. *Development* **131**, 1365-1375.

Development (2016) 143, 3742-3750 doi:10.1242/dev.130427

Khalsa, O., Yoon, J. W., Torres-Schumann, S. and Wharton, K. A. (1998). TGF-beta/BMP superfamily members, Gbb-60A and Dpp, cooperate to provide pattern information and establish cell identity in the Drosophila wing. *Development* **125**, 2723-2734.

Kunnapuu, J., Bjorkgren, I. and Shimmi, O. (2009). The Drosophila DPP signal is produced by cleavage of its proprotein at evolutionary diversified furin-recognition sites. *Proc. Natl. Acad. Sci. USA* **106**, 8501-8506.

Kunnapuu, J., Tauscher, P. M., Tiusanen, N., Nguyen, M., Löytynoja, A., Arora, K. and Shimmi, O. (2014). Cleavage of the Drosophila screw prodomain is critical for a dynamic BMP morphogen gradient in embryogenesis. *Dev. Biol.* **389**, 149-159.

Lapraz, F., Besnardeau, L. and Lepage, T. (2009). Patterning of the dorsal-ventral axis in echinoderms: insights into the evolution of the BMP-chordin signaling network. *PLoS Biol.* **7**, e1000248.

Le Good, J. A., Joubin, K., Giraldez, A. J., Ben-Haim, N., Beck, S., Chen, Y., Schier, A. F. and Constam, D. B. (2005). Nodal stability determines signaling range. *Curr. Biol.* **15**, 31-36.

Matsuda, S. and Shimmi, O. (2012). Directional transport and active retention of Dpp/BMP create wing vein patterns in Drosophila. *Dev. Biol.* **366**, 153-162.

McCabe, B. D., Marqués, G., Haghighi, A. P., Fetter, R. D., Crotty, M. L., Haerry, T. E., Goodman, C. S. and O'Connor, M. B. (2003). The BMP homolog Gbb provides a retrograde signal that regulates synaptic growth at the Drosophila neuromuscular junction. *Neuron* **39**, 241-254.

Misof, B. Liu, S. Meusemann, K. Peters, R. S. Donath, A. Mayer, C. Frandsen, P. B. Ware, J. Flouri, T. Beutel, R. G. et al. (2014). Phylogenomics resolves the timing and pattern of insect evolution. *Science* **346**, 763-767.

Nusslein-Volhard, C., Wieschaus, E. and Kluding, H. (1984). Mutations affecting the pattern of the larval cuticle in Drosophila melanogaster. I. Zygotic loci on the second chromosome. *Rouxs Arch. Dev. Biol.* **193**, 267-282.

Peter, I. S. and Davidson, E. H. (2011). Evolution of gene regulatory networks controlling body plan development. *Cell* **144**, 970-985.

Rafiqi, A. M., Park, C.-H., Kwan, C. W., Lemke, S. and Schmidt-Ott, U. (2012). BMP-dependent serosa and amnion specification in the scuttle fly Megaselia abdita. *Development* **139**, 3373-3382.

Reversade, B. and De Robertis, E. M. (2005). Regulation of ADMP and BMP2/4/7 at opposite embryonic poles generates a self-regulating morphogenetic field. *Cell* **123**, 1147-1160.

Saremba, S., Nickel, J., Seher, A., Kotzsch, A., Sebald, W. and Mueller, T. D. (2008). Type I receptor binding of bone morphogenetic protein 6 is dependent on N-glycosylation of the ligand. *FEBS J.* **27**, 172-183.

Schmoekel, H., Schense, J. C., Weber, F. E., Grätz, K. W., Gnägi, D., Müller, R. and Hubbell, J. A. (2004). Bone healing in the rat and dog with nonglycosylated BMP-2 demonstrating low solubility in fibrin matrices. *J. Orthop. Res.* **22**, 376-381.

Serpe, M., Umulis, D., Ralston, A., Chen, J., Olson, D. J., Avanesov, A., Othmer, H., O'Connor, M. B. and Blair, S. S. (2008). The BMP-binding protein Crossveinless 2 is a short-range, concentration-dependent, biphasic modulator of BMP signaling in Drosophila. *Dev. Cell* **14**, 940-953.

Shimmi, O. and Newfeld, S. J. (2013). New insights into extracellular and post-translational regulation of TGF-beta family signalling pathways. *J. Biochem.* **154**, 11-19.

Shimmi, O., Ralston, A., Blair, S. S. and O'Connor, M. B. (2005a). The crossveinless gene encodes a new member of the Twisted gastrulation family of BMP-binding proteins which, with Short gastrulation, promotes BMP signaling in the crossveins of the Drosophila wing. *Dev. Biol.* **282**, 70-83.

Shimmi, O., Umulis, D., Othmer, H. and O'Connor, M. B. (2005b). Facilitated transport of a Dpp/Scw heterodimer by Sog/Tsg leads to robust patterning of the Drosophila blastoderm embryo. *Cell* **120**, 873-886.

Sievers, F., Wilm, A., Dineen, D., Gibson, T. J., Karplus, K., Li, W., Lopez, R., McWilliam, H., Remmert, M., Soding, J. et al. (2011). Fast, scalable generation of high-quality protein multiple sequence alignments using Clustal Omega. *Mol. Syst. Biol.* **7**, 539.

Tamura, K., Stecher, G., Peterson, D., Filipski, A. and Kumar, S. (2013). MEGA6: molecular evolutionary genetics analysis version 6.0. *Mol. Biol. Evol.* **30**, 2725-2729.

van de Watering, F. C. J., van den Beucken, J. J. J. P., van der Woning, S. P., Briest, A., Eek, A., Qureshi, H., Winnubst, L., Boerman, O. C. and Jansen, J. A. (2012). Non-glycosylated BMP-2 can induce ectopic bone formation at lower concentrations compared to glycosylated BMP-2. *J. Control Release* **159**, 69-77.

Van der Zee, M., da Fonseca, R. N. and Roth, S. (2008). TGFbeta signaling in Tribolium: vertebrate-like components in a beetle. *Dev. Genes Evol.* **218**, 203-213.

Wang, Y.-C. and Ferguson, E. L. (2005). Spatial bistability of Dpp-receptor interactions during Drosophila dorsal-ventral patterning. *Nature* **434**, 229-234.

Werner, T., Koshikawa, S., Williams, T. M. and Carroll, S. B. (2010). Generation of a novel wing colour pattern by the Wingless morphogen. *Nature* **464**, 1143-1148.

Wotton, K. R., Alcaine Colet, A., Jaeger, J. and Jimenez-Guri, E. (2013). Evolution and expression of BMP genes in flies. *Dev. Genes Evol.* **223**, 335-340.

A

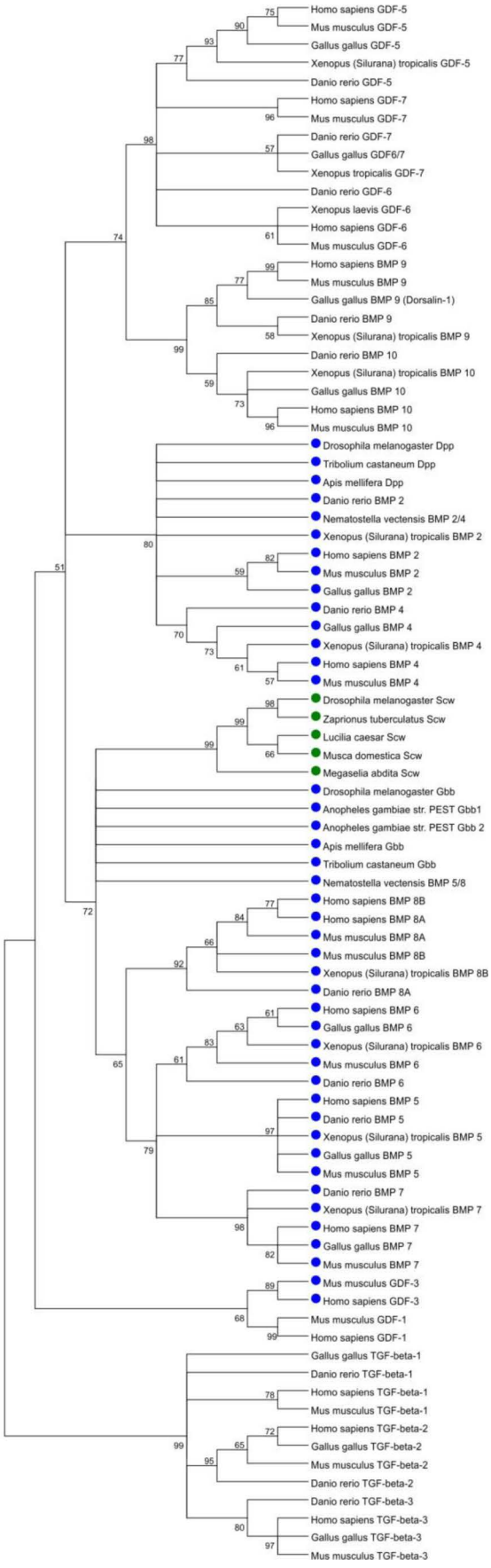

B

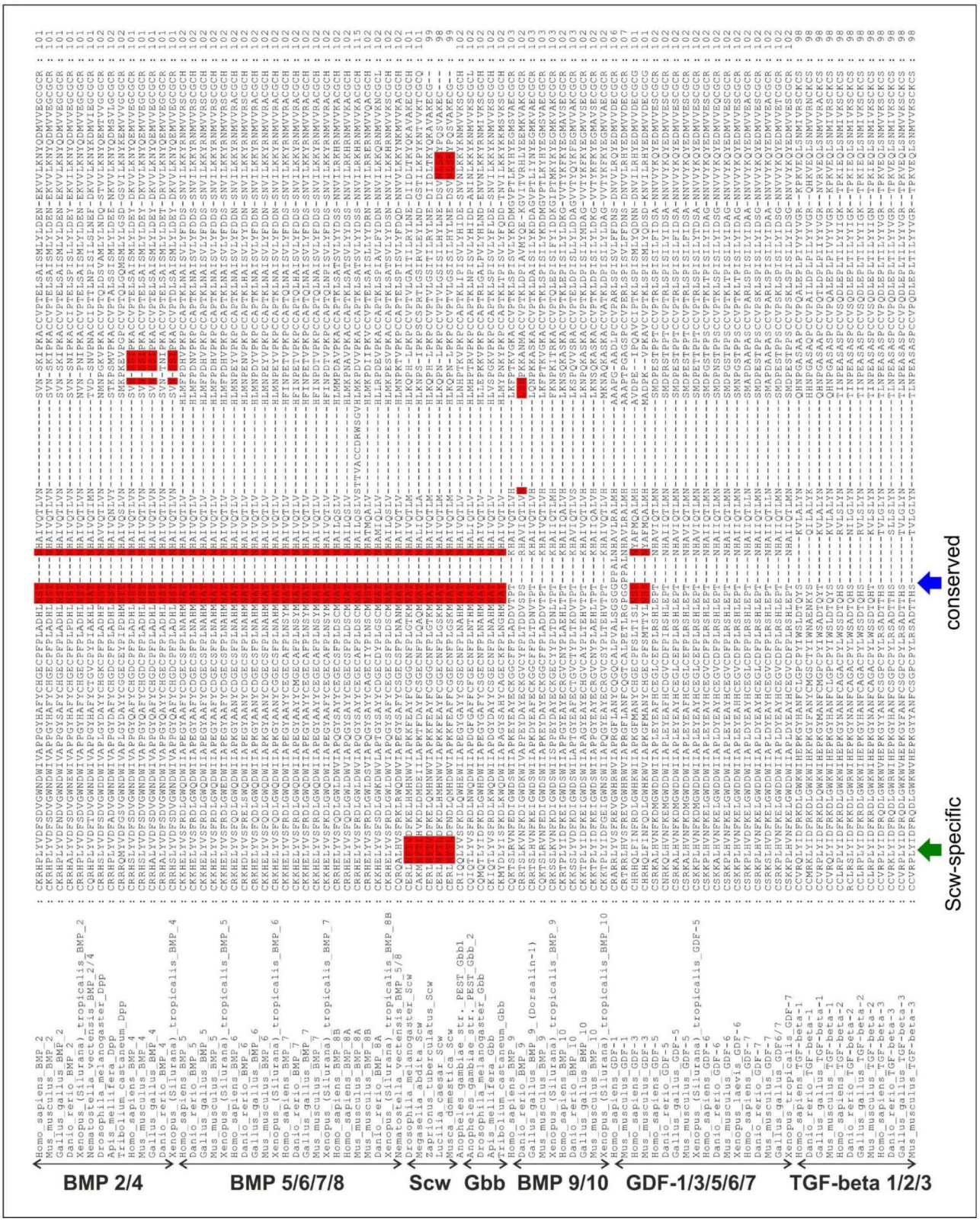

Fig. S1. Phylogenetic analysis of the TGF-β type ligands. (A) Molecular phylogenetic analysis of BMP- and GDF-type ligands by Maximum Likelihood method. The evolutionary history was inferred by using the Maximum Likelihood method based on the JTT matrix-based model (Jones et al., 1992). TGF-β 1/2/3 were used as outgroup. The percentage of trees in which the associated taxa clustered together is shown next to the branches and is based on 500 bootstrap trials. We used 50% as the cut-off value for condensing the tree. Branches supported by less than 50% are collapsed. The analysis involved 86 amino acid sequences (B). Blue dots indicate TGF-β type ligands comprising the conserved N-glycosylation motif. Green dots indicate Scw-type ligands including the Scw-specific N-glycosylation motif. (B) Amino acid multiple sequence alignment of various TGF-β-type ligand domains from different animal species. Amino acid sequence alignment of the conserved TGF-β ligand domain reveals a highly conserved N-glycosylation motif. N-glycosylation motifs are highlighted in red. The green arrow indicates the Scw-specific N-glycosylation motif. The blue arrow indicates the conserved, BMP-type ligand specific N-glycosylation motif. The alignment includes BMP2/4/Dpp, BMP5/6/7/8/Scw/Gbb, BMP9/10, GDF-1/3/5/6/7, and TGF-β type 1/2/3 ligand domains. Dashes are used to fill gaps. Reference numbers of the analyzed sequences can be found in Table S2.

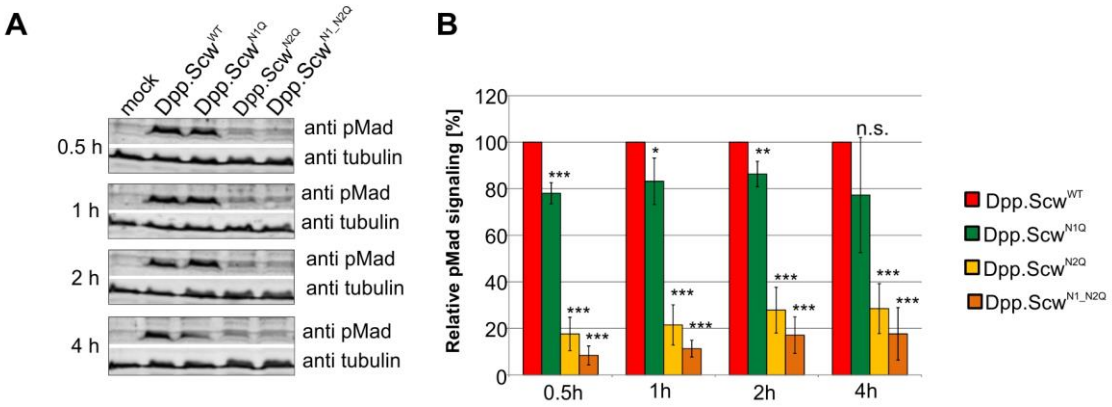

Fig. S2. Time-course of BMP signaling assay in *Drosophila* S2 cells. (A) Western blot analysis of a cell-based signaling assay in *Drosophila* S2 cells incubated with equivalent amount of either Dpp:Scw^{WT}, Dpp:Scw^{N1Q}, Dpp:Scw^{N2Q}, Dpp:Scw^{N1_N2Q}, or with PBS/0,1%BSA (mock). The pMad signal was measured at the time points 0.5, 1, 2, and 4 hours. Tubulin was used as an internal control. (B) Analysis of the Western blot shown in (A). The pMad intensity in Dpp:Scw^{WT} was calculated as 100%. Mock data were set to 0%. Data are obtained from five biological replicates, each performed in duplicates (n=5, graphs indicate means±95% CI, *$P\leq0.05$, **$P\leq0.01$, ***$P\leq0.001$, n.s., not significant. Significance was calculated by using the two-tailed Student's t-test.).

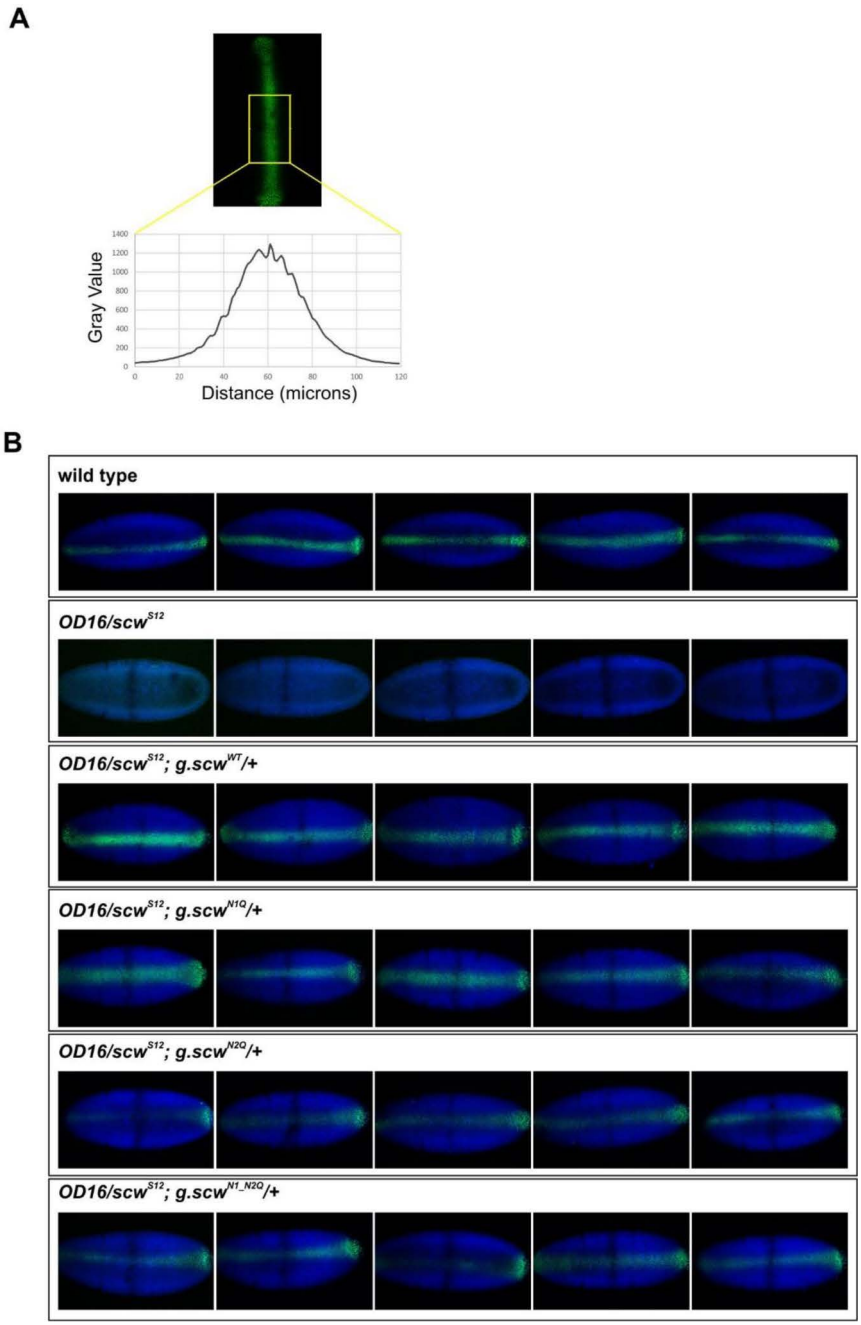

Fig. S3. Quantification of pMad signaling in *Drosophila* early embryos. (A) pMad intensity within a 120 x 200 µm rectangle was detected. The center of the rectangle was aligned with the the Kr-lacZ stripe (deriving from the *Df(2L)OD16, kr-lacZ* chromosome*).* (B) The pMad intensities of 5 embryos per genotype were measured for quantitative analysis (Fig. 3).

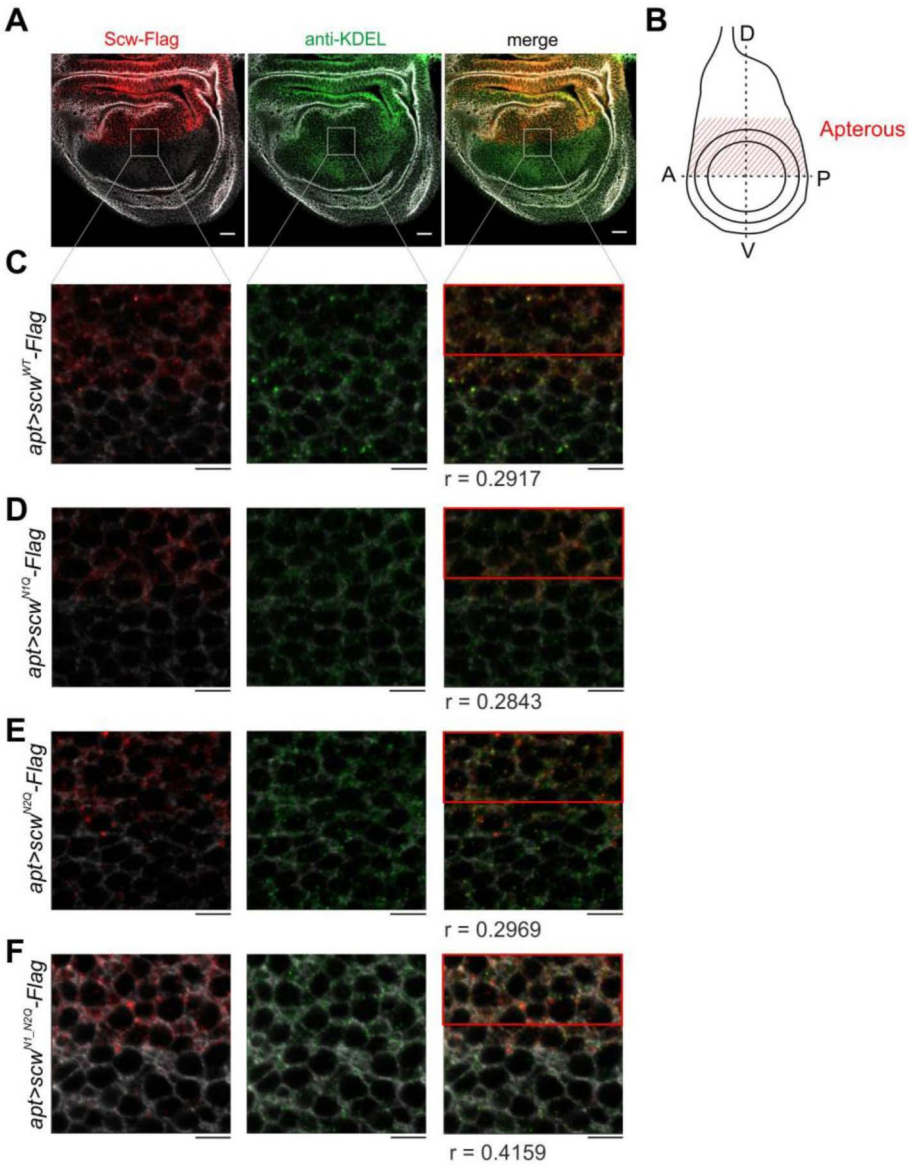

Fig. S4. Co-localization study of Scw glycosylation mutants with the endoplasmatic reticulum (ER) (A) Wing imaginal disc expressing *UAS-Scw^{WT}-Flag* under control of *apterous-Gal4* in the dorsal part of the wing disc. Grey squares highlight the approximate wing disc region shown in C-F. Flag (red), KDEL (green), and Scrib (white) were used for visualizing Scw ligands, ER, and cell membrane, respectively. (B) Schematic of the wing imaginal disc indicating the expression pattern of Apterous. (D – dorsal, V – ventral, A – anterior, P – posterior) (C-F) The pixel intensity correlation of the red and the green channel was analyzed for the region highlighted in the merged images. The corresponding Pearson's coefficient (r) is listed below the image. The images shown

are one section of a Z-stack through the wing imaginal disc. Scale bars in A = 20 µm. Scale bars in C-F = 5 µm.

Reference

Jones, D. T., Taylor, W. R. and Thornton, J. M. (1992). The rapid generation of mutation data matrices from protein sequences. *Computer applications in the biosciences : CABIOS* **8**, 275-282.

Table S1. Rescue experiment with transgenic flies.

	% of rescued flies carrying 1 copy of the rescue construct *OD16/scw^{S12};g.scw/+* [a]					% of rescued flies carrying 2 copies of the rescue construct *OD16/scw^{S12};g.scw/ g.scw* [a]				
	OD16/ scw^{S12}	***g.scw^{WT}***	***g.scw^{N1Q}***	***g.scw^{N2Q}***	***g.scw^{N1_N2Q}***	***OD16/ scwS^{12}***	***g.scw^{WT}***	***g.scw^{N1Q}***	***g.scw^{N2Q}***	***g.scw^{N1_N2Q}***
1	0.0 (35)	112.8 (61)	11.1 (57)	0.0 (47)	0.0 (37)	0.0 (49)	88.9 (13)	71.4 (57)	0.0 (11)	6.5 (32)
2	0.0 (52)	80.0 (63)	18.2 (36)	0.0 (39)	0.0 (44)	0.0 (54)	133.3 (40)	70.8 (65)	0.0 (26)	40.0 (12)
3	0.0 (51)	61.5 (51)	36.8 (45)	0.0 (34)	0.0 (35)	0.0 (50)	50.0 (10)	153.2 (83)	22.2 (10)	0.0 (20)
4	0.0 (51)	60.6 (43)	28.6 (48)	0.0 (11)	0.0 (33)	0.0 (72)	106.7 (23)	122.2 (58)	0.0 (20	6.3 (33)
5	0.0 (54)	88.9 (52)	48.6 (46)	0.0 (24)	0.0 (47)	0.0 (45)	105.3 (29)	94.4 (53)	0.0 (13)	0.0 (25)
6	0.0 (40)	120.9 (69)	32.3 (36)	0.0 (52)	0.0 (52)	0.0 (64)	171.4 (26)	56.0 (64)	6.7 (31)	100.0 (15)
7	0.0 (46)	133.3 (20)	47.5 (73)	0.0 (17)	0.0 (47)	0.0 (65)	271.4 (33)	66.7 (56)		13.3 (16)
8	0.0 (58)	126.3 (62)	40.0 (72)	0.0 (31)	0.0 (26)	0.0 (53)	110.0 (31)	66.7 (56)		0.0 (29)
9	0.0 (50)	87.8 (59)	43.9 (50)	0.0 (49)	0.0 (32)	0.0 (37)	123.1 (42)	54.8 (79)		0.0 (22)
10	0.0 (41)	68.4 (51)	40.0 (66)	0.0 (27)		0.0 (54)	280.0 (24)	95.5 (65)		0.0 (24)
11	0.0 (47)	53.8 (33)	71.4 (38)	0.0 (52)		0.0 (47)	158.3 (43)	128.9 (74)		0.0 (30)
12	0.0 (50)	100.0 (36)	27.3 (50)	5.1 (40)		0.0 (46)		88.5 (88)		
13	0.0 (41)	116.1 (49)	102.7 (56)	0.0 (38)		0.0 (9)		76.2 (87)		
14	0.0 (50)	90.9 (64)	15.1 (57)	4.3 (47)		0.0 (61)		113.6 (69)		
15	0.0 (44)	41.9 (52)		0.0 (37)				88.2 (49)		
16	0.0 (53)	95.2 (31)		0.0 (42)				74.5 (70)		
17	0.0 (54)	77.4 (43)		0.0 (38)				68.0 (67)		
18	0.0 (42)	109.1 (34)		0.0 (45)						
19	0.0 (38)									
Σ [b]	19	18	14	18	9	14	11	17	6	11

[a] Number of counted flies is shown in parentheses. [b] Total amount of analysed crosses. 20 crosses were set for each genotype (1 virgin female/cross).

Table S2. Reference numbers of the TGF-β type ligands used in the phylogentic analysis

	Species	NCBI Reference	GenBank	UniProtKB/ Swiss-Prot
1	*Homo sapiens*	NP_001191.1		
2	*Mus musculus*	NP_031579.2		
3	*Gallus gallus*	NP_989689.1		
4	*Danio rerio*	NP_571435.1		
5	*Xenopus (Silurana) tropicalis*	NP_001015963.1		
6	*Nematostella vectensis*		AAR13362.1	
7	*Drosophila melanogaster*		AAN10431.1	
8	*Megaselia abdita*		AFK24733.1	
9	*Apis mellifera*	XP_006569849.1		
10	*Tribolium castaneum*	NP_001034540.1		
11	*Homo sapiens*	NP_001193.2		
12	*Mus musculus*	NP_031580.2		
13	*Gallus gallus*	NP_990568.3		
14	*Danio rerio*	NP_571417.1		
15	*Xenopus (Silurana) tropicalis*	NP_001017034.2		
16	*Homo sapiens*			P22003.1
17	*Danio rerio*	NP_957345.1		
18	*Gallus gallus*	NP_990479.1		
19	*Mus musculus*	NP_031581.2		
20	*Xenopus (Silurana) tropicalis*	XP_002934893.1		
21	*Homo sapiens*			P22004.1
22	*Danio rerio*	NP_001013357.1		
23	*Gallus gallus*	XP_418956.4		
24	*Mus musculus*	NP_031582.1		
25	*Xenopus (Silurana) tropicalis*	NP_001106378.1		
26	*Homo sapiens*			P18075.1
27	*Danio rerio*	NP_001070614.1		
28	*Mus musculus*	NP_031583.2		
29	*Gallus gallus*	XP_417496.4		
30	*Xenopus (Silurana) tropicalis*	NP_989197.1		
31	*Homo sapiens*	NP_861525.2		
32	*Mus musculus*	NP_001242948.1		
33	*Danio rerio*	NP_001038436.1		
34	*Homo sapiens*			P34820.2
35	*Mus musculus*	NP_031585.2		
36	*Xenopus (Silurana) tropicalis*	XP_002941697.1		
37	*Nematostella vectensis*		ABC88372.1	
38	*Megaselia abdita*		AFK24736.1	
39	*Drosophila melanogaster*	NP_001286088.1		
40	*Zaprionus tuberculatus*		ADR57149.1	
41	*Lucilia caesa*		ADR57151.1	
42	*Musca domestica*		ADR57152.1	
43	*Anopheles gambiae str. PEST*	XP_316789.3		
44	*Anopheles gambiae str. PEST*	XP_320599.3		
45	*Drosophila melanogaster*	NP_001286786.1		
46	*Apis mellifera*	XP_394252.2		
48	*Tribolium castaneum*	NP_001107813.1		
47	*Homo sapiens*			Q9UK05.1
48	*Danio rerio*	NP_001165057.1		
49	*Gallus gallus*	NP_990763.1		
50	*Mus musculus*	NP_062379.3		
51	*Xenopus (Silurana) tropicalis*	XP_002940692.2		
52	*Homo sapiens*			O95393.1
53	*Danio rerio*	NP_001124072.1		
54	*Gallus gallus*	NP_001264975.1		
55	*Mus musculus*	NP_033886.2		
56	*Xenopus (Silurana) tropicalis*	XP_002935357.1		
57	*Homo sapiens*	NP_001483.		
58	*Mus musculus*	NP_032133.2		
59	*Homo sapiens*	NP_065685.1		
60	*Mus musculus*	NP_032134.2		
61	*Homo sapiens*			P43026.3
62	*Danio rerio*	XP_002662587.1		
63	*Gallus gallus*	NP_989669.1		

64	*Mus musculus*	NP_032135.2		
65	*Xenopus (Silurana) tropicalis*	NP_001128589.1		
66	*Homo sapiens*			Q6KF10.1
67	*Danio rerio*	NP_001153466.1		
68	*Mus musculus*	NP_038554.1		
69	*Xenopus laevis*			Q9W753
70	*Homo sapiens*			Q7Z4P5.2
71	*Danio rerio*	XP_694563.2		
72	*Mus musculus*	NP_038555.1		
73	*Gallus gallus*			O93573
74	*Xenopus tropicalis*			F6Z923
75	*Homo sapiens*			P01137.2
76	*Danio rerio*	NP_878293.1		
77	*Gallus gallus*		AFD30526.1	
78	*Mus musculus*	NP_035707.1		
79	*Homo sapiens*			P61812.1
80	*Danio rerio*	NP_919366.1		
81	*Gallus gallus*	NP_001026216.2		
82	*Mus musculus*	NP_033393.2		
83	*Homo sapiens*			P10600.1
84	*Danio rerio*	NP_919367.2		
85	*Gallus gallus*	NP_990785.1		
86	*Mus musculus*	NP_033394.2		